9.2 EM PROPAGATION OVER THE OCEAN: ANALYSIS OF RED EXPERIMENT DATA

Tihomir Hristov[1*] and Carl Friehe[2]
[1]*Department of Earth and Planetary Sciences, Johns Hopkins University*
[2]*Department of Mechanical and Aerospace Engineering, University of California, Irvine*

1. Introduction

The pattern of electromagnetic signals propagation over the ocean is a combined result of atmospheric refraction and scattering from the rough ocean surface. The vertical gradients of the averaged atmospheric humidity and temperature can lead to a gradient of the air's refractivity, thus creating a refractive duct in the marine atmospheric boundary layer. Normal modes waveguide models (Hitney et al. (1985); Bass and Fuks (1979); Wait (1970)) have been developed to describe the signal propagation in ducting conditions. However, previous observations as well as results from this experiment (Anderson et al. (2003)) have shown that the available models tend to overestimate the detected signal intensity at the receiver. To address such discrepancy we need accurate information regarding the refractivity profiles in the marine atmospheric boundary layer. Thus the first hypothesis to be tested is whether the duct is too "weak" to confine the radiation from escaping into space. Other physical processes capable of degrading the energy of the EM signal and contracting its coherence radius are the scattering from the turbulent inhomogeneities of the atmospheric refractive index as well as scattering from the rough ocean surface (Ishimaru (1978); Rytov et al. (1987)). Of particular interest is the influence of the ocean surface waves, a distinct element of the marine environment, on the EM propagation.

2. Rough Evaporation Duct (RED) Experiment

Our measurements during Rough Evaporation Duct (RED) Experiment took place 10km North of Oahu, Hawaii on the stable instrument platform *FLIP* (Fig. 1) and lasted between August 23 and September 19, 2001. The goal of the field experiment was to collect data for the structure of the atmospheric refractive index over the ocean as well as about the statistics of the surface waves. Air's refractive index n is a function of air's and water vapor densities and can be obtained from measurements of atmospheric pressure P, temperature T and humidity Q (Bean and Dutton (1966)). To capture both slow and fast variability of the atmospheric refractive index and wind velocity, we used chilled mirror (EdgeTech Vigilant) and Lyman-α hygrometers, thermistors (Hart Scientific) and ultrasonic anemometers/thermometers (CSAT3, Campbell Scientific, Gill Instruments). Atmospheric pressure was registered through complementary measurements from a barometer coupled with a differential pressure transducer. The dynamic pressure fluctuations were eliminated by the design of the barometer's inlet. The instruments were deployed at five levels along a mast from *FLIP* (Fig. 1). Wave elevation was measured directly beneath the mast. The slight motion of the platform was recorded as signals of accelerations and angular rates (Systron Donner MotionPak and Boeing CMIGITS II). Data were collected continuously. Wherever possible, the signals were sampled at 50Hz. Throughout the experiment wind speed was moderate and within the range between 5 and 10$\mathrm{m/s}$. The ocean was persistently warmer than the air by about 1$^\circ\mathrm{C}$. The waves standard deviation $\langle\eta^2\rangle^{1/2}$ did not exceed 0.5m.

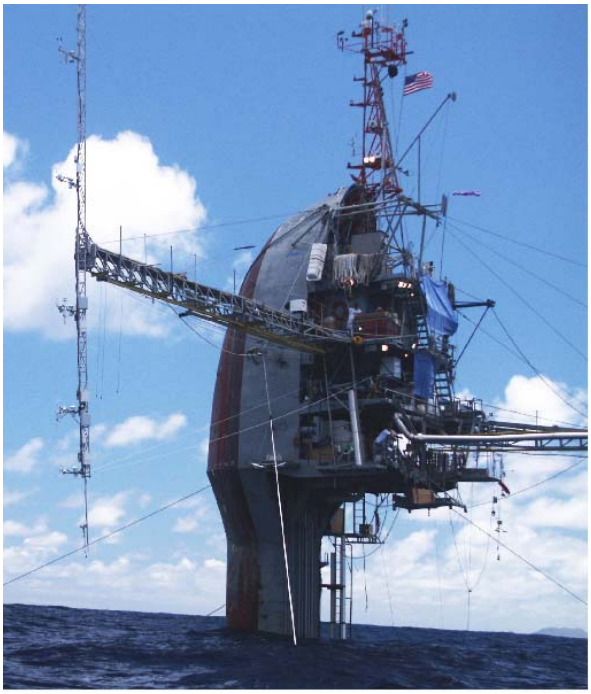

Figure 1: The Floating Instrument Platform *(FLIP)* during the experiment. Instruments measuring wind velocity, air temperature and humidity, and atmospheric pressure, are seen on the mast at five heights. Wave surface elevation is measured beneath the mast.

*Corresponding author address: Tihomir Hristov, Department of Earth and Planetary Sciences, Johns Hopkins University, Baltimore, Maryland 21218, e-mail: Tihomir.Hristov@jhu.edu

3. Refractive index fluctuations

The motion of the air in the atmospheric boundary layer is key to understanding the fluctuations of the refractive index over the ocean. Sweeps and ejections are coherent structures commonly occurring in turbulent boundary layers (Robinson (1991)). They displace sizable parcels of air upward (ejections) or downward (sweeps) in the marine boundary layer. In the case of negative gradients of temperature (when the ocean is warmer than air) and humidity, the ejections bring warmer and more humid air upward while sweeps bring cooler and dryer air downward. Both disturb the average distribution of the refractive index. Multiple events of ejections can be observed in the signals from RED. However, the intermittent nature of these events makes them difficult to identify by some clear criterion without requiring visual inspection of the data. We are currently working on obtaining their statistics and inferring their influence on the electromagnetic propagation pattern.

Of special interest is the signature of the ocean surface waves, distinguishing the oceanic environment of EM propagation. The structure and the dynamics the marine atmospheric boundary layer is profoundly affected by the waves, which deform the mean wind flow streamlines. The kinematics of that deformation can be described in terms of the critical layer theory (Miles (1957)). Considering a single wave mode, the air flow induced by it can be predicted (Fig. 2). The air flow induced by a spectrum of ocean waves is a Fourier superposition of the flows shown in (Fig. 2).

In the presence of gradients of the atmospheric humidity and temperature, the deformation of the streamlines displaces the sheared profiles of these quantities and leads to wave-induced fluctuations of the atmospheric refractive index. As a result, EM signals propagating over the ocean encounter a semi-periodic refractive structure, which along with the turbulence can degrade signal's energy (Tatarskii (1992)). The wave-induced fluctuations of the refractive index are unique to the oceanic environment. Their structure function does not follow the power 2/3 scaling law (Ishimaru (1978)), valid for turbulent fluctuations, and thus their influence should be studied separately.

The concept of analytic signal is helpful for understanding both the wave-induced fluctuations in the air as well as the scattering properties of the ocean surface. Consider the signal obtained from point measurement of the ocean surface elevation $\eta(t)$. Its analytic counterpart is

$$\zeta(t) = \eta(t) + \mathrm{i}[\eta(t) * (1/t)] = A(t)e^{\mathrm{i}\Phi(t)} \qquad (1)$$

where $\eta(t) * (1/t)$ stands for the convolution of $\eta(t)$ with $1/t$, also known as the Hilbert transform of the signal $\eta(t)$. The analytic signal allows ascribing to the signal $\eta(t)$ an instantaneous amplitude $A(t)$ and phase $\Phi(t)$ for each point in time, as defined in (1).

We can assume that the quantity X measured above the waves (X standing for wind velocity, temperature, humidity or pressure) consists of mean, turbulent and wave-induced components $X = \overline{X} + X' + \widetilde{X}$. The separation of the wave-induced fluctuations $\widetilde{X}$ from the turbulent background X' is necessary before they can be analyzed. The conditional expectation of a signal with respect to the phase of waves $\left\langle X - \overline{X} | \Phi \right\rangle$, suppresses the turbulence in $(X - \overline{X})$ and emphasizes the wave-correlated component $\widetilde{X}$ (Hristov et al. (1998)). Although in general the conditional average $\left\langle X - \overline{X} | \Phi \right\rangle$ is not identical to $\widetilde{X}$, it is representative for the amplitude and the phase (referenced to the phase of the waves) of $\widetilde{X}$. We will be interested by the wave-induced fluctuations of along-wind $\tilde{u}$ and vertical $\tilde{w}$ velocity, revealing the deformation of the wind streamlines over the ocean, and the resulting from that wave-induced fluctuations of temperature $\widetilde{T}$ and humidity $\widetilde{Q}$. $\widetilde{T}$ and $\widetilde{Q}$, in turn, cause the wave-induced fluctuations of the refractivity $\widetilde{N}$.

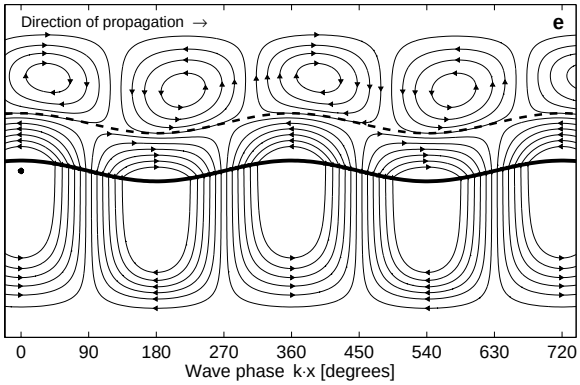

Figure 2: Wave induced flow streamlines, according to the critical layer theory of Miles (1957). The solid line is the air-water interface and the dashed line is the critical height, where the mean wind speed equals the phase speed of the wave mode.

Figure 3 summarizes the wave-driven dynamics of the atmospheric boundary layer, as detected by the instruments at the lowest mast level, 5.1m from the ocean surface. The ultrasonic anemometer provided the wind velocities. The temperature was recovered by superimposing the low frequency variability from the thermistor with the fast fluctuations from the ultrasonic thermometer, corrected for the presence of water vapor. Humidity signal came from the chilled mirror hygrometer, whose slow response leads to a distortion (lower amplitude and phase lag) of the true humidity fluctuations. As for radio frequencies the humidity provides the largest contribution in the refractive variability (Bean and Dutton (1966)), the distortions of the humidity measurements are also present in the estimates of the atmospheric refractivity. The conditional averages of along-wind $\langle u - \overline{u} | \Phi \rangle$ and vertical $\langle w - \overline{w} | \Phi \rangle$ velocities, biased toward the dominant long-wave spectral components, are closely consistent with the predictions of the critical layer theory of Miles (1957). Figure 3 shows how the oscillating ocean surface forces the profiles of along-wind velocity, temperature and hu-

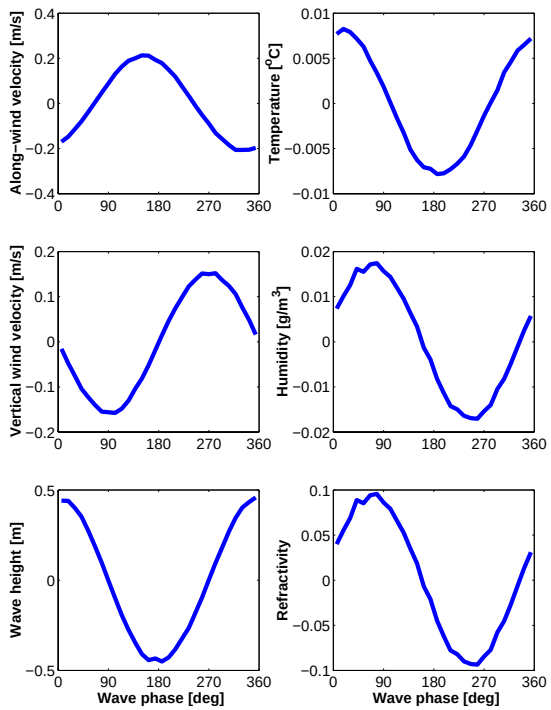

Figure 3: Conditional averages for the along-wind $\langle u-\overline{u}|\Phi\rangle$ and vertical $\langle w-\overline{w}|\Phi\rangle$ wind velocities, wave elevation $\langle\eta|\Phi\rangle$, temperature $\langle T-\overline{T}|\Phi\rangle$, humidity $\langle Q-\overline{Q}|\Phi\rangle$, and refractivity $\langle N-\overline{N}|\Phi\rangle$. All the signals are obtained from instruments at the lowest level, 5.1m from the mean ocean surface.

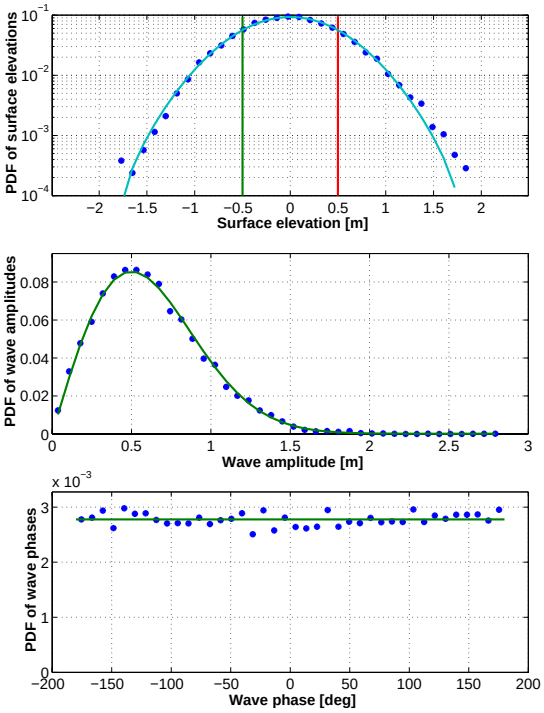

Figure 4: Probability density distributions of surface elevation $p(\eta)$ (upper plot), wave amplitude $p(A)$ (middle plot), and wave phase $p(\Phi)$ (lower plot). The vertical lines in the upper plot indicate the waves standard deviation $\pm\langle\eta^2\rangle^{1/2}$.

midity leading to fluctuations of the refractivity. In the case of negative vertical gradient of temperature (i.e. when the ocean is warmer than the air) an upward displacement of the surface and the wind's streamlines causes higher temperature at a fixed height over the wave crests. Same response to the wave forcing (i.e. higher humidity at fixed height over the wave crests) should be expected from the signal of humidity, and consequently, by the refractivity. The deviation from such behavior for the humidity and refractivity in Fig. 3, likely results from the signal distortion inherent to the chilled mirror hygrometer. A comparison between the variances of the humidity signal $\langle(Q-\overline{Q})^2\rangle$ from the chilled mirror hygrometer and an open path infrared hygrometer (LI-COR LI-7500, a fast response instrument) shows 30% lower variance for the signal from the chilled mirror hygrometer.

4. Reexamining a model for ocean surface scattering

In ducting conditions, when the EM signal grazes the ocean, propagation and surface scattering become inextricably coupled (Barrick (1998)). The model of Miller et al. (1984), describing the intensity of the coherent signals scattered from the ocean surface, has been aimed to improving the accuracy of previous models (Isakovich (1952); Ament (1953)). The predictions of Miller et al. (1984) have been incorporated in models for propagation in a duct (Hitney (1999)). However, the assumptions used in Miller et al. (1984) appear to be verifiably inconsistent with our current knowledge about the statistics of the ocean surface and warrant reexamination of that model. Namely, Miller et al. (1984) propose that the sea surface can be divided into a large number of domains where the surface elevation is a sine wave with a random amplitude and phase $\eta = A\sin\Phi$. The amplitude A is prescribed to have a Gaussian probability distribution

$$p(A) = (\sqrt{2\pi}\sigma_A)^{-1}\exp[-A^2/(2\sigma_A^2)], \qquad (2)$$

while the phase Φ is assumed to be uniformly distributed over the interval $[-\pi/2, \pi/2]$. Miller et al. (1984) conclude that a zero-order modified Bessel function must correct the coherent signal intensity obtained earlier by Isakovich (1952); Ament (1953):

$$R = \exp(-g)\, I_0(g), \qquad (3)$$

where $g = (\kappa\sigma_\eta \sin\gamma)^2$, $\kappa = 2\pi/\lambda$ is the EM signal's wave number, σ_η is the standard deviation of the of the ocean surface elevation, γ is the grazing angle.

Ignoring the nonlinear dynamics of the surface waves, the ocean surface is a superposition of Fourier modes

with random phases. For such superposition, as justified by the central limit theorem, even small number of modes converge to a surface with normally distributed elevations, i.e. $p(\eta) = (\sqrt{2\pi}\sigma_\eta)^{-1} \exp[-\eta^2/(2\sigma_\eta^2)]$. Recalling the definition (1), the amplitude A is obtained to have Rayleigh distribution (Longuet-Higgins (1957)):

$$p(A) = (A/\sigma_\eta^2) \exp[-A^2/(2\sigma_\eta^2)]. \quad (4)$$

Such a conclusion has been supported by experiments and our results are no exception. Figure 4 shows experimentally obtained probability density distributions and analytic curves (Gaussian for the wave elevations $p(\eta)$, Rayleigh for the amplitudes $p(A)$ and constant for the wave phases $p(\Phi)$) that best approximate them.

Although Miller et al. (1984) claim that the factor $I_0(g)$ in (3) brings better agreement with the experiment of Beard (1961), the above considerations indicate that such agreement cannot validate the model of Miller et al. (1984). We need to point out, that the independent measurements of Karasawa and Shiokawa (1988) have been too scattered to support or reject the factor $I_0(g)$.

Consequently, the Bessel function factor $I_0(g)$ in (3) appears unnecessary, which in turn leads to lower intensity for the reflected coherent signals. In the context of discussion in Hitney (1999), the scattering from the rough surface can account for more energy losses in propagation models, e.g. MLAYER (Hitney et al. (1985)).

Acknowledgments

We gratefully acknowledge the expert assistance of *FLIP*'s captain Tom Golfinos and crew provided to us during the RED experiment and the support through ONR N00014-00-1-0137 and ONR N00014-00-1-0120. George Elizarraras and Roberto Ku contributed to this project with engineering expertise.

References

Ament, W. S.: 1953, Toward a theory of reflection by a rough surface. *Proc. IRE*, **41**, 142–146.

Anderson, K., P. Frederickson, and E. Terrill: 2003, Air-Sea Interaction Effects on Microwave Propagation over the Sea During the Rough Evaporation Duct (RED) Experiment. *12th ISA*, 9-13 February, Long Beach, CA, Paper 9.1.

Barrick, D. E.: 1998, Grazing behavior of scatter and propagation above any rough surface. *IEEE Transactions on Antennas and Propagation*, **46**, 73–83.

Bass, F. G. and I. M. Fuks: 1979, *Wave Scattering from Statistically Rough Surfaces*, volume 93 of *International Series of Natural Philosophy*. Pergamon, Oxford.

Bean, B. and E. Dutton: 1966, *Radio Meteorology*. National Bureau of Standarts Monograph 92, Washington, DC.

Beard, C. I.: 1961, Coherent and incoherent scattering of microwaves from the ocean. *IEEE Transactions on Antennas and Propagation*, **AP-9**, 470–483.

Hitney, H.: 1999, Evaporation duct propagation and near-grazing angle scattering from a rough sea. *Proceedings IGARSS*, Hamburg, Germany, 28 June to 2 July 1999.

Hitney, H. V., J. H. Richter, R. A. Rappert, K. D. Anderson, and G. B. Baumgartner: 1985, Tropospheric radio propagation assesment. *Proc. IEEE*, **73**, 265–283.

Hristov, T., C. Friehe, and S. Miller: 1998, Wave-coherent fields in air flow over ocean waves: Identification of cooperative behavior buried in turbulence. *Phys. Rev. Letters*, **81**, 5245–5248.

Isakovich, M. A.: 1952, Wave scattering from a statistically rough surface. *Journal of Theoretical and Experimental Physics, (ZhETF)*, **23**, 305–314.

Ishimaru, A.: 1978, *Wave propagation and scattering in random media*. Academic Press, New York.

Karasawa, Y. and T. Shiokawa: 1988, A simple prediction method for l-band multipath fading in rough sea conditions. *IEEE Transactions on Communications*, **36**, 1098–1104.

Longuet-Higgins, M. S.: 1957, The statisical analysis of a random, moving surface. *Philosophical Transactions of the Royal Society of London*, **249**, 321–387.

Miles, J. W.: 1957, On the generation of surface waves by shear flows. *J. Fluid Mech.*, **3**, 185–204.

Miller, A. R., R. M. Brown, and E. Vegh: 1984, New derivation for the rough-surface reflection coefficient and for the distribution of the sea-wave elevations. *IEE Proceedings, Part H*, volume 131(2), 114–116.

Robinson, S. K.: 1991, Coherent motions in the turbulent boundary layer. *Annual Review of Fluid Mechanics*, **23**, 601–639.

Rytov, S. M., Y. A. Kravtsov, and V. I. Tatarskii: 1987, *Priciples of statistical radiophysics 4: Wave propagation through random media*. Springer-Verlag, Heidlberg.

Tatarskii, V. I.: 1992, Review of scintillation phenomena. *Wave propagation in random media (Scintillation)*, V. I. Tatarskii, A. Ishimaru, and V. Zavorotny, eds., SPIE — The international Society of Optical Engineering, Copublished by SPIE Press and Institute of Physics Publishing, Philadelphia, 2–15.

Wait, J. R.: 1970, *Electromagnetic waves in stratified media*. Pergamon, Oxford.